It's all about the talus - *In vivo* tarsal joint complex kinematics during walking, running, and hopping

Behling, Anja-Verena[1,2]; Welte, Lauren[3]; Kelly, Luke[1,4,5]; Rainbow, Michael J[2]

[1]School of Human Movement and Nutrition Science, The University of Queensland, Brisbane, Australia

[2]Department of Mechanical and Materials Engineering, Queen's University, Kingston, Canada

[3]Mechanical Engineering, University of Wisconsin-Madison, Wisconsin United States

[4]Griffith Centre of Biomedical & Rehabilitation Engineering, Griffith University, Gold Coast, Australia

[5]School of Health Sciences & Social Work, Griffith University, Gold Coast, Australia

a.behling@uq.edu.au

ORCID # 0000 0003 0844 4143

Key words biplanar videoradiography, helical axis of motion, foot function

Competing Interest

AVB, LW, MR, and LK declare that they have no conflict of interest. AVB is supported by the International Society of Biomechanics Matching Dissertation Grant. LW is funded by the Natural Sciences and Engineering Research Council Postdoctoral Fellowship (NSERC PDF: 558140-2021). MR is funded by the Natural Sciences and Engineering Research Council of Canada Discover Grant (RGPIN/04880-2022) and LK by the Australian Research Council Discover Early Career Research Award (DE200100585).

Abstract

The interaction among joints of the tarsal complex (talus, navicular, calcaneus, and cuboid) plays an essential role in locomotor function; however, its anatomical and functional complexity poses substantial challenges in quantifying its motion. We determine the mobility of these joints across locomotion tasks and investigate whether the individual kinematic tarsal joint axes align with the talus morphology.

We use highly accurate biplanar videoradiography to obtain three-dimensional bone kinematics. We calculate each tarsal bone's rotation axis and compare these axes to each other and to a coordinate system embedded in the talus capturing the morphological subtalar joint axis. We measure the total rotation about and the orientation of the rotation axes in the subtalar joint direction for the landing and propulsion phases, respectively.

The rotation axes of all three bones relative to the talus closely align with each other and with the morphological subtalar joint axis. This suggests that the tarsal complex's motion might be described by one common axis in the non-pathological population. The ranges of motion about this axis differed among the bones.

Our results provide a novel perspective of healthy foot function across different locomotion tasks underscoring the importance of understanding tarsal motion with respect to subject-specific morphology.

1. Introduction

The human midtarsal joint complex is comprised of the talonavicular, and the calcaneocuboid joints. The movement of these joints and the subtalar joint (calcaneus relative to talus) – defined collectively as the tarsal complex (midtarsal and subtalar joints) – plays an important role in facilitating bipedal gait [1–5]. However, capturing *in vivo* tarsal joint motion is challenging. The rare data that has been captured has been interpreted using the unproven framework that the foot becomes rigid during push-off [6]. In addition, there is large variation in bone shape that has the potential to modify tarsal complex function [7–10]. A new approach investigating the tarsal complex under a new framework that views the foot as a highly mobile functional unit, while accounting for the underlying morphology may provide new insights into foot function.

Recent studies of tarsal bone motion suggest that the tarsal complex behaves as a functional unit during bipedal gait [11–15]. They found that motion of the talonavicular, calcaneocuboid, and subtalar joints is synchronous and homodromous (rotating in the same direction) in all three planes, which implies that the joints rotate around a common functional axis. However, the functional axis during locomotor tasks has not been directly measured in vivo [16]. Understanding the motion of the tarsal complex in terms of functional axes is useful for two reasons: first, it allows us to compare bone motions directly, independent of coordinate systems; second, the functional axis is presumably tied to the underlying bone morphology, which can provide insight into the relationship between morphology and function. We aim to understand if the synchronous and homodromous motion of the tarsal complex extends to other locomotion tasks and to quantify the alignment of the functional axes during these tasks.

A morphological axis defined by the calcaneus and navicular facets on the talus is likely a good candidate for capturing the functional axis of the tarsal complex [8,16 p. 617 ff]. We define this morphological axis as the morphological subtalar axis because it is thought to align with the subtalar rotation axis [8,16 p. 617ff]. If tarsal complex motion occurs about a functional axis, we expect the motion of the navicular and cuboid relative to the talus to also occur about the morphological subtalar axis. This analysis deviates from previous work that examines talonavicular and calcaneocuboid motion independently [5,11,13,19]. Our rationale here is that it has been shown previously that the navicular and cuboid move as a unit [11–15]. Analyzing their motion relative to the talus allows us to directly test whether this is the case.

Understanding whether the tarsal complex behaves as a functional unit and how its function relates to morphology may allow researchers to determine which shape features are important to human gait and the evolution of bipedalism. Moreover, recent statistical shape modeling studies [28–32] highlighted substantial morphological variations of non-pathological human tali. These shape variations have considerable influence on the talonavicular and subtalar joint facets [8,10,20]. Hence, if morphological features in these facets change, so might the morphological axis and therefore the rotational and functional axes and resulting kinematics. Understanding these tarsal complex form-function relationships will allow scientists and clinicians to better understand the role of an individual's anatomy, or changes to it, in the onset and progression of pathology.

The purpose of this study was to determine if 1) tarsal motion occurs about a common functional axis across a range of locomotor tasks and 2) whether the individual tarsal joint axes align with the morphological axis of the subtalar joint. We utilize highly accurate biplanar videoradiography (BVR) technology to obtain bone kinematics and calculate each bone's motion, relative to the talus, using the helical axis of motion approach to represent the functional axis [21].

2. Methodology

2.1. Overview and Participants

Kinematic data were combined from two separate data collections and study protocols for this study. All participants provided written informed consent (MECH-061-17 and MECH-063-18).

Walking and running data was obtained from nine healthy participants (5 females; mean ± std; mass 76.1 ± 15.8 kg; height 171.1 ± 15.8 cm; 20.0 ± 6.8 years) with no history of lower limb injury. Participants walked and ran at self-selected speeds while wearing minimalist shoes (Xero, Prio). BVR data was collected from the right leg of each participant (125 Hz for walking, 250 Hz for running, range of 70-80 kV, 100-125 mA). Ground reaction force data were collected simultaneously using two force plates (1125 Hz, AMTI Optima, AMTI, Watertown, MA), whose forces were combined and synchronized to the BVR system via a trigger step function. We analyzed one gait cycle per condition from three collected trials for each participant. The field of view for the BVR system is relatively small, so the foot bones of interest were not always visible for the entire stance phase. Therefore, each trial was screened for the maximal number of frames in which the bones were visible to obtain as much data as possible (~85-100% of stance; Supplement Figure S1).

In addition to walking and running, we captured unilateral hopping. Hopping was chosen because it produces a large range of cyclical motion about the ankle and tarsal joints [22,23] and can be captured within the small field of view of the BVR system. For the hopping data, nine healthy subjects (5 females; mean ± std, mass 71.3 ± 14.5 kg; height 171.4 ± 10.7 cm; 27.6 ± 7.4 years) with no history of lower limb injury provided written informed consent to participate in this study. Participants hopped barefoot on their right leg at a frequency of 156 beats per minute, guided by a metronome. The BVR system (125 Hz, range of 70–80 kV, 100–125 mA) and force plate data were collected simultaneously (1125Hz, AMTI Optima, AMTI, Watertown, MA) and manually synchronized to the BVR system using optical motion capture (Qualysis Track Manager, Goeteborg, Sweden). Three hops with the entire foot in the field of view were kept for further processing.

2.2. Data Processing: Kinematics Derived from Biplanar Videoradiography

A computed tomography scan (CT, 120 kV, 60mA, model: Lightspeed 16, n = 11, Revolution HD, n = 1, General Electric Medical Systems, USA) was obtained from the right foot while participants were lying in a prone position (average resolution: 0.356 x 0.356 x 0.625 mm). Talus, navicular, calcaneus, and cuboid bones were segmented to create three-dimensional bone models (Mimics 24.0, Materialise, Leuven, Belgium). Subsequently, bone surface meshes and partial volumes were generated, and digitally reconstructed radiographs were created [24].

The processing pipeline for foot BVR data can be found in our earlier research [25,26]. Briefly, the high-speed cameras were calibrated using a custom calibration cube, and the images were undistorted in XMALab (Brown University, USA) [27,28]. The translation and orientation of the bones of interest were measured by tracking partial volumes representing each bone of interest using Autoscoper (Brown University, USA) [24].

Gait events were defined using a 15 N threshold in the vertical ground reaction force to determine foot contact and take-off during locomotion. Because each of the locomotion tasks has two distinctly different directions of motion (landing and propulsion), we divided ground contact in two different phases (landing and push-off). For walking and running, midstance was determined as the zero crossing of the anterior-posterior ground reaction force. For hopping, midstance was determined as the maximal vertical ground

reaction force after the passive peak of the vertical ground reaction force curve (active peak). Landing describes the phase from foot contact to midstance. Push-off is defined from midstance to take off.

We implemented a morphological coordinate system for the talus (Figure 1) [29,30]. The primary axis (*z*-axis) was defined by fitting two spheres, one to the navicular facet and the other to the calcaneus facet on the talus. The morphological subtalar joint axis (z-axis) was defined by the vector that connected the centroids of each sphere and oriented superiorly [31]. The y-axis was the mutual perpendicular of the long axis of a cylinder fit to the talar dome and the z-axis. Lastly, the x-axis was calculated as the cross product of the y- and z- axes. The origin lies on the cylinder axis where the distance to the subtalar vector line is minimal (Figure 1).

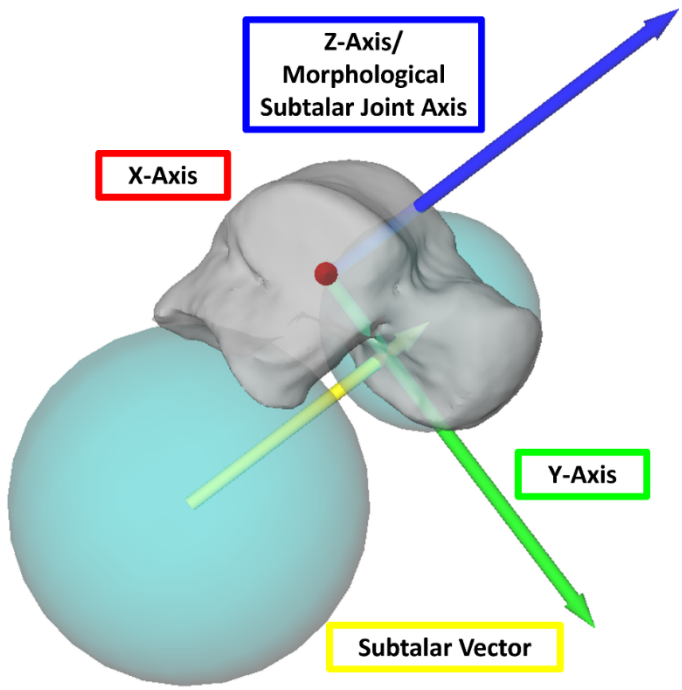

Figure 1: Right talus; lateral view. Example subtalar coordinate system in the talus. X-axis is red (oriented out of the page), y-axis green (inferiorly oriented) and z-axis blue (morphological subtalar joint axis; oriented superiorly). The subtalar joint axis is parallel to the vector connecting the centroids of the sphere fits of the talonavicular and subtalar facet (teal spheres). The origin is defined on the cylinder line and the point where the distance to the vector connecting the subtalar vector (yellow arrow).

Helical axes of motion were calculated for the bones of interest [21]. Briefly, the helical axis of motion represents the change in position and orientation of one rigid body moving relative to a mathematically fixed rigid body – here, the talus. It defines an axis in space, termed the rotation axis, that the moving body rotates about and translates along. In this study, we focus on the orientation of the rotation axis in z-direction and the angle swept out by the moving body as it rotates about the rotation axis (total rotation).

We calculated the rotation axis and angle of the subtalar joint (calcaneus relative to talus), talonavicular joint (navicular relative to talus), and talocuboid joint (cuboid relative to talus) and resolved the axis in the talus coordinate system (Figure 2). Each gait phase (landing and push-off) corresponds to one rotation axis, which was calculated between the frames determined as touchdown and midstance and between midstance and take-off, respectively. If a helical axis reported total rotation ≤5° or if the bone (typically the cuboid) was occluded by other bones during tracking, we excluded this trial of the bone for the participant from further analysis. If bones were not trackable at touchdown or push-off, we used the next available frame in order to calculate the landing and push-off phase, respectively.

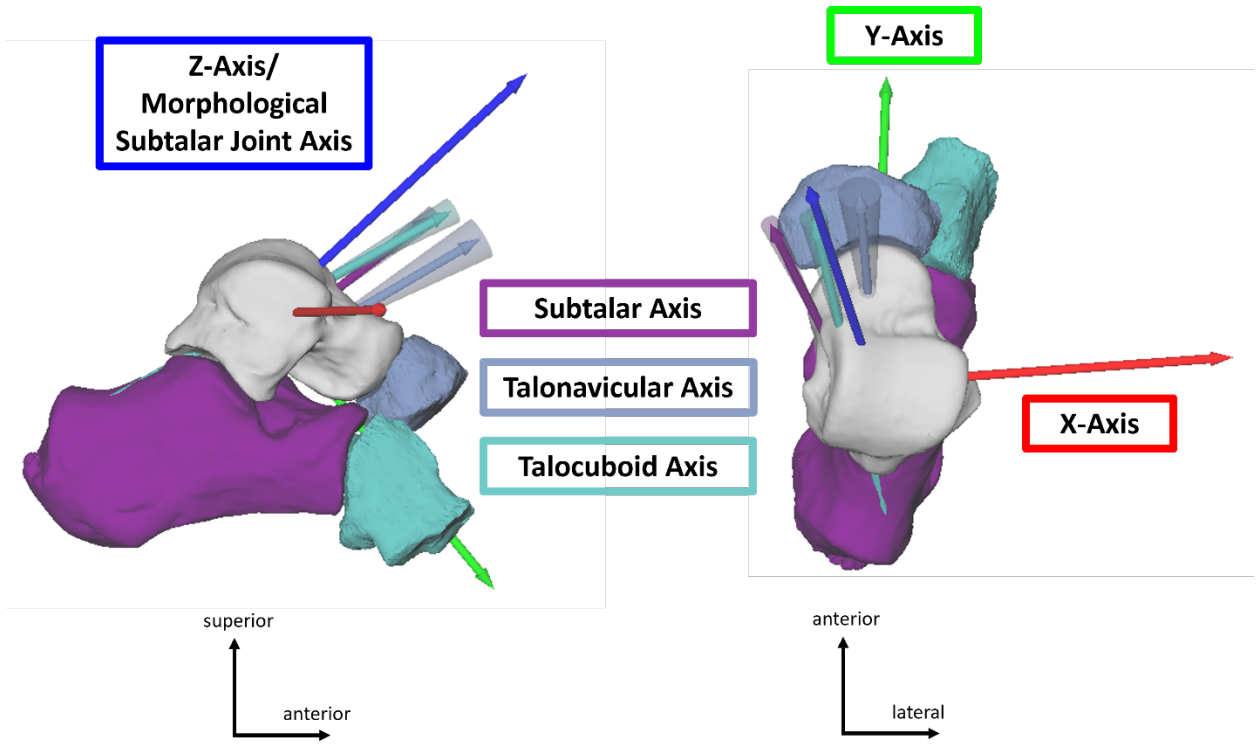

Figure 2: Right foot. Representative rotation axes of motion for the push-off phase during hopping for all three joints (subtalar in purple, talonavicular in blue, and talocuboid in teal) relative to the talus (for $n_{Participants}$ = 1). Helical axes are indicated as arrows with their standard deviation displayed as cones about each axis. The subtalar coordinate system is indicated in red (x-axis), green (y-axis) and blue (z-axis/ morphological subtalar joint axis).

1.1. Analysis

As the statistical power is limited in small data sets and we are interest in similarity measures, tests for statistical differences are not ideal. We explain our reasoning behind the statistical tests in the following, yet statistical values should be viewed with caution and are exploratory.

To determine whether the rotation axes are similarly oriented, we performed one-way ANOVAs as a proxy for similarity measures (absence of difference) for the z-axis orientation component of the rotation axes of the three joints relative to each other (Supplement Table S1-3). Additionally, we created Bland-Altman plots as a measure of similarity to test whether the three rotation axes agree in their orientation in z-direction (Supplement Figure S2-4).

To determine whether the rotation axes were aligned with the morphological subtalar axis, we again examined the z-component of the rotation axes' orientation, which corresponded to the morphological subtalar axis direction. If a rotation axis orientation has a value of 1 in the subtalar joint direction (z-direction), it means that the rotation axis is perfectly aligned with the morphological subtalar joint axis (same orientation), and all its motion is occurring about this axis.

To examine whether the navicular and cuboid moved as a unit relative to the talus, and whether their motion was greater than subtalar motion as shown previously, we performed one-way ANOVAs comparing the magnitude of total rotations across the different bones.

Differences between landing and push-off regarding total rotation magnitudes and orientation in the *z*-axis per joint were determined using paired t-tests for each mode of locomotion and joint.

Non-parametric equivalents were used whenever assumptions of paired t-tests or ANOVAs were not met. The significance level was set to 0.05 and adjusted when required using a Bonferroni correction.

3. Results

Since there were no differences between landing and push-off in total rotation and orientation for any of the three bones for all three locomotion tasks ($p \geq 0.039$, alpha = 0.0176), we only report push-off results. Please refer to the supplements for landing (Supplement Figures S2-7, Tables S1-3).

Despite large variation in ranges of motion across joints and participants (Figure 3), we found that all three rotation axes were largely aligned with each other across locomotor modes (Figure 4 & 5, Supplement Figures 2-4). Across locomotor modes, the calcaneus consistently rotated substantially less than the cuboid or navicular (Table 1). These results were significant for hopping (calcaneus rotates significantly less than the cuboid and navicular; $p \leq 0.0078$, Supplement Table S3) and running (calcaneus rotates significantly less than the navicular; $p = 0.0039$, Supplement Table S2). The navicular and cuboid showed no significant differences in their rotations (Figure 5 & Table 1), despite the cuboid consistently rotating on average about 2-3° (range -9 – 1°) less than the navicular across locomotor modes and while rotating about similar rotation axes.

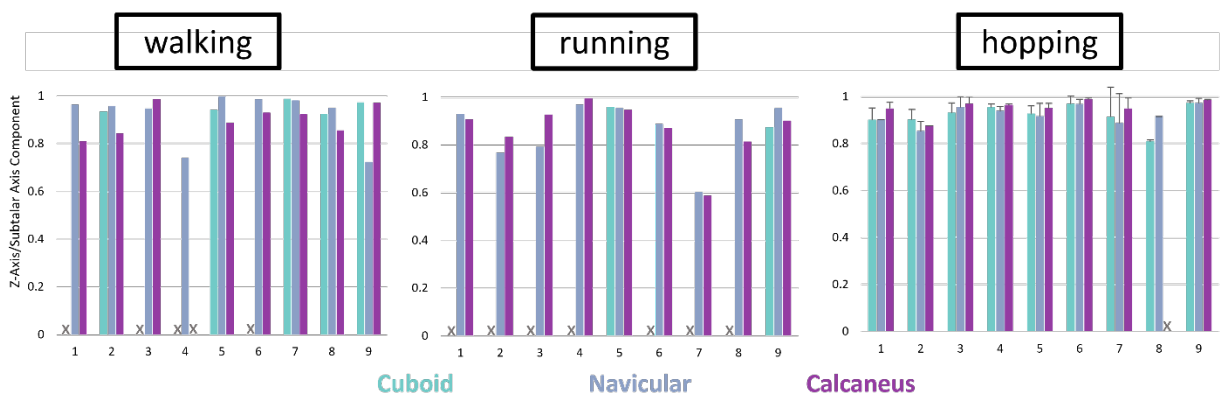

Figure 3: Total rotation in degrees during push-off phase of different modes of locomotion for the talocuboid (cuboid; teal), talonavicular (navicular; blue), and subtalar (calcaneus; purple) joints for all participants ($n_{Participants} = 9$; $n_{Trials_walk/run} = 1$; $n_{Trials_hopping} = 3$). Participants' total rotation for some bones might be missing if the bone could not be tracked or was ≤ 5° in these instances there is no data presented in the graphs (indicated with an X).

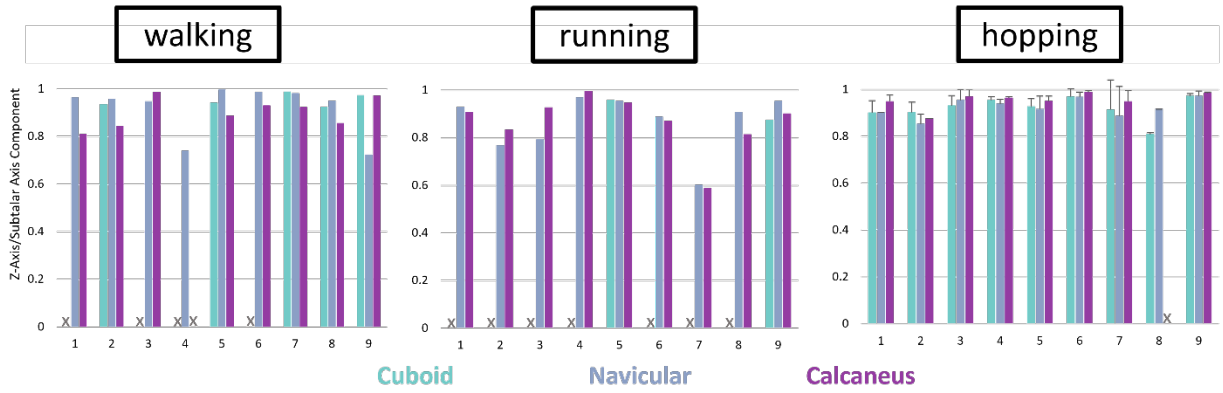

Figure 4: Orientation of helical axis of motion in the subtalar axis direction (z-axis) during push-off phase of different modes of locomotion for the talocuboid (cuboid; teal), talonavicular (navicular; blue), and subtalar (calcaneus; purple) joints for all participants ($n_{Participants} = 9$; $n_{Trials_walk/run} = 1$; $n_{Trials_hopping} = 3$). Participants' orientation values for some bones might be missing if the bone could not be tracked or was ≤ 5° in these instances there is no data presented in the graphs (indicated with an X).

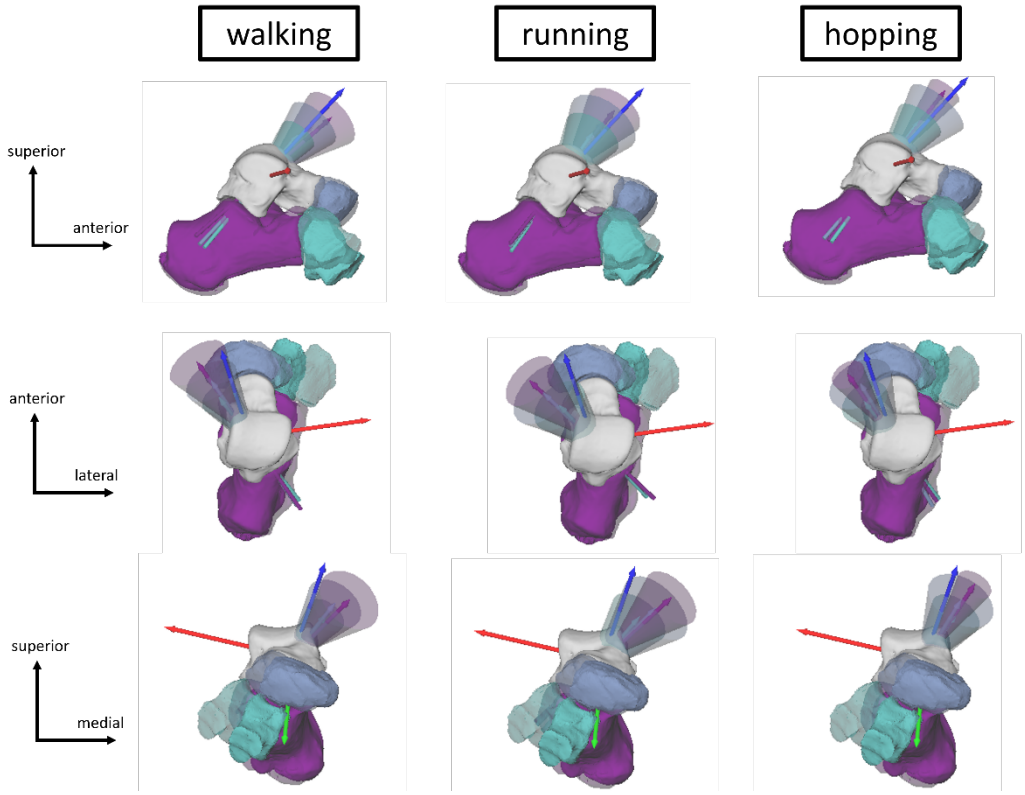

Figure 5: Orientation of helical axis of motion during push-off across different modes of locomotion (columns) for the talonavicular (navicular; blue), talocuboid (cuboid; teal), and subtalar (calcaneus; purple) joints across all participants ($n_{Participants} = 9$). The cone reflects the standard deviation across participants. For visual purposes each axis and cone have different lengths(calcaneus > navicular > cuboid). The subtalar coordinate system is reflected in red, green, and blue (x-, y-, z-axis respectively). Transparent bones indicate position of bones during midstance while solid bones indicate position of bones during toe-off. Different perspectives are visualized in the rows.

Table 1: Mean (standard deviation) of total rotation and z-component of the rotation axes of the talonavicular (navicular), talocuboid (cuboid), and subtalar (calcaneus) joints during push-off.

	Total Rotation (°)			**Morphological Subtalar Joint Alignment**		
	Walking	Running	Hopping	Walking	Running	Hopping
Navicular	19.5 (9.2)	19.5 (5.0)	15.4 (4.3)	0.92 (0.11)	0.86 (0.12)	0.92 (0.04)
Cuboid	17.1 (9.1)	16.8 (1.0)	13.7 (3.8)	0.95 (0.03)	0.91 (0.06)	0.92 (0.05)
Calcaneus	10.8 (4.0)	10.4 (3.6)	10.0 (2.2)	0.90 (0.06)	0.86 (0.12)	0.95 (0.03)

We also found that most of each joint's motion occurred about the morphological subtalar axis (Figure 4 & 5), with average orientation magnitudes ranging from 0.86 to 0.95 (Table 1). In other words, approximately 90% of the total rotation of the talonavicular, talocuboid, and subtalar motion occurs about the morphological subtalar axis.

4. Discussion

The objective of our study was to determine if the tarsal complex behaves as a functional unit across locomotor modes and if its motion is consistent with talus articular morphology. To accomplish our objectives, we used highly accurate BVR equipment to measure bone morphology in motion during walking, running, and hopping. We found that the subtalar, talonavicular, and talocuboid joint axes are closely aligned with each other and with the morphological subtalar joint axis across both gait phases in walking, running, and hopping. Although the amount of rotation differed among bones, these findings indicate that the tarsal complex behaves as a single functional unit that is driven by talus articular surface morphology. This behavior cannot be seen by analyzing all three joints independently and with individual coordinate systems. Our findings are not surprising for the calcaneus and navicular, which directly articulate with the talus. However, it is noteworthy that the cuboid is separated from the talus by the calcaneus, yet still primarily rotates relative to the talus about the subtalar axis. This suggests that using the talus as a common reference bone for midtarsal complex motion might be a good indicator of non-pathological locomotion patterns.

All bones displayed substantial magnitudes of rotation about the subtalar axis (z-direction) during walking, running, and hopping. Interestingly, despite sharing a common axis of motion, the three bones exhibited differing magnitudes of rotation, and high levels of inter-subject variation. Our findings are consistent with previous bone-pin and BVR studies showing that the navicular and cuboid move largely as a functional unit [11–14], with the caveat that the navicular rotates on average 12% more than the cuboid during the propulsion phase. Additionally, we observed that the navicular and cuboid bones display substantially greater magnitudes of rotation than the calcaneus during propulsion (~35-60% more depending on locomotion type), which is similar to previous literature [12,13,15]. These data contrast with Elftman and Manter's [17] suggestion that the tarsal complex locks (i.e. does not move) when the talonavicular and calcaneocuboid joint axes converge from midstance to push-off, converting the foot into a "rigid" or stiff lever for propulsion. Others have also demonstrated that the tarsal complex does not lock [11–13,19] and our results further strengthen the evidence against midtarsal locking or stiffening during propulsion.

We are intrigued by our findings that the navicular, cuboid, and calcaneus rotate different amounts about a common axis that is defined by subtalar and talonavicular joint facet morphology. Since the talocuboid and subtalar joint motions are less than talonavicular motion (particularly the subtalar joint), we speculate that these joints may be constraining the navicular's motion path relative to the talus. Since the talonavicular has been described as an elliptical paraboloid articulation [32], it is reasonable to assume it possesses more potential degrees of freedom than the saddle-shaped articular surfaces of the calcaneocuboid and subtalar joints [17]. We believe this system may be analogous to the engineering design of a dual track slider, where one groove has a tight tolerance to define the motion (subtalar joint and to a lesser degree the calcaneocuboid joint) and the second groove has a looser tolerance and is deemed the follower (talonavicular joint). This configuration is advantageous because it prevents the entire dual track slider from locking. Hence, the navicular might be adjusting and potentially compensating for limited motion of the other joints as necessary. That said, this navicular-follower analogy remains speculative and requires further exploration, as we cannot determine cause and effect with these methods.

The morphology of a bone's articular surface is often assumed to be a key determinant of how that bone or joint moves during locomotion; however, osseus morphology is rarely considered in dynamic evaluation of human foot function [22,33,34]. Recent statistical shape modelling (morphometrics) studies of the human tarsal bones have highlighted the marked inter-subject variability in the shape of the tarsal bone articular surface [8,10]. Whilst we have not directly evaluated shape in this study, our morphological axis approach does account for some of this shape variability among individuals. It is possible that variations in shape (and joint axis orientations) may explain the wide inter-subject variation in the magnitude of rotation, with particular shape features enabling greater, or restricted rotation about a common functional axis. We did not control for walking and running speeds in our study, so it is also likely that variation in gait speed may also contribute to varying magnitudes of rotation. However, we controlled for frequency in hopping, and the intra-individual consistency in rotation magnitude between walking, running, and hopping suggests this may be minimal. For example, individuals who reported lower rotation magnitudes in walking typically also reported lower rotation magnitudes in running. Understanding the contributing factors to inter-subject variability is important for clinicians and anthropologists when determining boundaries for healthy versus pathological tarsal complex function, planning clinical treatments, or when comparing tarsal kinematics across species.

4.1. Limitations

The acquisition and processing of data using BVR is time-intensive, which is why our sample size is relatively small. Due to the limited field of view and the stationary setup of the BVR, it is not possible to repeatedly capture the entire stance phase for all foot bones during walking and running, resulting in missing data. However, we were able to capture more than 90% of stance on average (Supplement Figure S1), which should suffice for most biomechanical and clinical applications. Moreover, bone occlusion, which refers to bony overlap in the capture volume, can make bone tracking challenging or impossible, particularly in the midfoot region. These limitations make it difficult to provide a complete dataset of cuboid kinematics for each mode of locomotion and participant. Therefore, researchers may need to prioritize which bones are imaged to address their research question and optimize their BVR setup accordingly.

4.2. Clinical and Future Application

Based on the findings presented here, we speculate that morphological variations in subtalar and talonavicular joint articular surfaces may have substantial effects on the alignment of the morphological subtalar joint axis and, thus, the kinematics of the entire tarsal complex. Hence, changes in osseous structure occurring due to conditions such as osteoarthritis may lead to a progressive sequence of structural and functional impairments. At the opposite end of the lifespan, it is also possible that developmental plasticity

associated with childhood (and lifetime) physical activity may also play a considerable role in how our feet function through adulthood into our elderly years. Moreover, this uniaxial representation of the tarsal complex might simplify future implant design in subtalar joint replacements or talus arthroplasties as according to our results subtalar morphology is directly related to tarsal kinematics and therefore mobility.

Lastly, looking at tarsal complex kinematics relative to the talus might be an approach to distinguish healthy from pathological tarsal complex function instead of interpreting joint motion independently (e.g., calcaneocuboid joint). This would streamline the interpretation of tarsal complex kinematics and clearly identify individuals with deviating functional axes and therefore movement patterns. Moreover, the talus morphology of clinical populations might differ from a healthy population, which would be reflected in the morphological talus coordinate system as well as the motion, which could be evaluated with the herein mentioned approach.

5. Conclusion

We have shown that the calcaneus, navicular, and cuboid bones move about a common axis that coincides with the morphological subtalar joint axis during walking, running, and hopping. Furthermore, we observed substantial tarsal complex movement during landing and push-off in different modes of locomotion, suggesting a considerable degree of mobility throughout the stance phase. Lastly, our results underscore the importance of understanding both tarsal motion and morphology and the potential implications for developing targeted foot treatments for pathological gait characteristics.

6. References

1. Crompton RH, Pataky TC, Savage R, D'Août K, Bennett MR, Day MH, et al. Human-like external function of the foot, and fully upright gait, confirmed in the 3.66 million year old Laetoli hominin footprints by topographic statistics, experimental footprint-formation and computer simulation. J R Soc Interface. 2012;9(69):707–19.

2. Venkadesan M, Yawar A, Eng CM, Dias MA, Singh DK, Tommasini SM, et al. Stiffness of the human foot and evolution of the transverse arch. Nature. 2020;579(7797):97–100.

3. Jung D, Mun K-R, Yoo S, Jung H, Kim J. A Study on the Contribution of Medial and Lateral Longitudinal Foot Arch to Human Gait. In: 2021 43rd Annual International Conference of the IEEE Engineering in Medicine & Biology Society (EMBC). 2021. p. 4559–65.

4. Kelly LA, Lichtwark G, Cresswell AG. Active regulation of longitudinal arch compression and recoil during walking and running. J R Soc Interface. 2015;12(102):20141076.

5. Vogler HW, Bojsen-Møller F. Tarsal functions, movement, and stabilization mechanisms in foot, ankle, and leg performance. J Am Podiatr Med Assoc. 2000 Mar;90(3):112–25.

6. Behling A-V, Rainbow MJ, Welte L, Kelly LA. A Narrative Review: Chasing footprints in time – Reframing our understanding of human foot function in the context of current evidence and emerging insights. Biol Rev. 2023;12999.

7. Lenz AL, Krähenbühl N, Peterson AC, Lisonbee RJ, Hintermann B, Saltzman CL, et al. Statistical shape modeling of the talocrural joint using a hybrid multi-articulation joint approach. Sci Rep. 2021;11(1):7314.

8. Krähenbühl N, Lenz AL, Lisonbee RJ, Peterson AC, Atkins PR, Hintermann B, et al. Morphologic analysis of the subtalar joint using statistical shape modeling. J Orthop Res. 2020 Dec 7;38(12):2625–33.

9. Liu T, Jomha NM, Adeeb S, El-Rich M, Westover L. Investigation of the Average Shape and Principal Variations of the Human Talus Bone Using Statistic Shape Model. Front Bioeng Biotechnol. 2020;8:656.

10. Melinska AU, Romaszkiewicz P, Wagel J, Antosik B, Sasiadek M, Iskander DR. Statistical shape models of cuboid, navicular and talus bones. J Foot Ankle Res. 2017 Jan 31;10(1):6.

11. Lundgren P, Nester CJ, Liu A, Arndt A, Jones R, Stacoff A, et al. Invasive in vivo measurement of rear-, mid- and forefoot motion during walking. Gait Posture. 2008;28(1):93–100.

12. Arndt A, Wolf P, Liu A, Nester CJ, Stacoff A, Jones R, et al. Intrinsic foot kinematics measured in vivo during the stance phase of slow running. J Biomech. 2007;40(12):2672–8.

13. Wolf P, Stacoff A, Liu A, Nester CJ, Arndt A, Lundberg A, et al. Functional units of the human foot. Gait Posture. 2008 Oct 1;28(3):434–41.

14. Okita N, Meyers SA, Challis JH, Sharkey NA. Midtarsal joint locking: new perspectives on an old paradigm. J Orthop Res. 2014;32(1):110–5.

15. Chen Wang MD, Geng X, Wang S, Xin Ma MD, Xu Wang MD, Jiazhang Huang MD, et al. In vivo kinematic study of the tarsal joints complex based on fluoroscopic 3D-2D registration technique. Gait Posture. 2016 Sep;49:54–60.

16. Lundberg A, Svensson OK. The axes of rotation of the talocalcaneal and talonavicular joints. Foot. 1993;3(2):65–70.

17. Elftman H, Manter JT. The Evolution of the Human Foot, with Especial Reference to the Joints. J Anat. 1935;70(Pt 1):56–67.

18. Fick R. Handbuch der Anatomie und Mechanik der Gelenke unter Berücksichtigung der bewegenden Muskeln: Spezielle Gelenk- und Musckelmechanik. Jena: Gustav Fischer Verlag; 1911.

19. Arndt A, Westblad P, Winson I, Hashimoto T, Lundberg A. Ankle and subtalar kinematics measured with intracortical pins during the stance phase of running. Foot Ankle Int. 2004;25(5):357–64.

20. Nozaki S, Watanabe K, Kamiya T, Katayose M, Ogihara N. Morphological variations of the human talus investigated using three-dimensional geometric morphometrics. Clin Anat. 2020;

21. Panjabi MM, Krag MH, Goel VK. A technique for measurement and description of three-dimensional six degree-of-freedom motion of a body joint with an application to the human spine. J Biomech. 1981;14(7):447–60.

22. Kessler SE, Lichtwark GA, Welte LKM, Rainbow MJ, Kelly LA. Regulation of foot and ankle quasi-stiffness during human hopping across a range of frequencies. J Biomech. 2020;108:109853.

23. Birch J V, Kelly LA, Cresswell AG, Dixon SJ, Farris DJ. Neuromechanical adaptations of foot function to changes in surface stiffness during hopping. J Appl Physiol. 2021 Feb 11;130(4):1196–204.

24. Miranda DL, Schwartz JB, Loomis AC, Brainerd EL, Fleming BC, Crisco JJ. Static and dynamic error of a biplanar videoradiography system using marker-based and markerless tracking techniques. J Biomech Eng. 2011 Dec 31;133(12):121002.

25. Kessler SE, Rainbow MJ, Lichtwark GA, Cresswell AG, D'Andrea SE, Konow N, et al. Kessler, 2019 - Direct Comparison of biplanar videoratiography and optical motion capture for foot and ankle kinematics.pdf. Frontiers in Bioengineering and Biotechnology Frontiers Media S.A.; Aug 23, 2019 p. 199.

26. Welte L, Dickinson A, Arndt A, Rainbow MJ. Biplanar Videoradiography Dataset for Model-based Pose Estimation Development and New User Training. JoVE. 2022;(183):e63535.

27. Knörlein BJ, Baier DB, Gatesy SM, Laurence-Chasen JD, Brainerd EL. Validation of XMALab software for marker-based XROMM. J Exp Biol. 2016 Dec 1;219(23):3701–11.

28. Brainerd EL, Baier DB, Gatesy SM, Hedrick TL, Metzger KA, Gilbert SL, et al. X-ray reconstruction of moving morphology (XROMM): precision, accuracy and applications in comparative biomechanics research. J Exp Zool Part A Ecol Genet Physiol. 2010 Jun 1;313A(5):262–79.

29. Conconi M, Pompili A, Sancisi N, Leardini A, Durante S, Belvedere C. New anatomical reference systems for the bones of the foot and ankle complex: definitions and exploitation on clinical conditions. J Foot Ankle Res [Internet]. 2021;14(1):66. Available from: https://doi.org/10.1186/s13047-021-00504-5

30. Modenese L, Renault J-B. Automatic generation of personalised skeletal models of the lower limb from three-dimensional bone geometries. J Biomech. 2020;116:110186.

31. Parr WCH, Chatterjee HJ, Soligo C. Calculating the axes of rotation for the subtalar and talocrural joints using 3D bone reconstructions. J Biomech. 2012 Apr;45(6):1103–7.

32. Mann R. Biomechanics of the foot. In: Atlas of Orthotics: biomechanical principles and application. Mosby; 1975. p. 257–66.

33. Kern AM, Papachatzis N, Patterson JM, Bruening DA, Takahashi KZ. Ankle and midtarsal joint quasi-stiffness during walking with added mass. PeerJ. 2019;2019(9):1–17.

34. McDonald KA, Stearne SM, Alderson JA, North I, Pires NJ, Rubenson J. The role of arch compression and metatarsophalangeal joint dynamics in modulating plantar fascia strain in running. PLoS One. 2016;11(4):e0152602.